MnGaPO-2: Synthesis and Characterization of $[MnGa(PO_3OH)_2(PO_4)][C_6N_2H_{14}]$, a New Microporous Manganese−Gallium Phosphate

Ann M. Chippindale,* Andrew D. Bond, and Andrew R. Cowley

Chemical Crystallography Laboratory, University of Oxford, 9 Parks Road, Oxford OX1 3PD, U.K.

Anthony V. Powell

Department of Chemistry, Heriot-Watt University, Riccarton, Edinburgh E14 4AS, U.K.

Received March 21, 1997. Revised Manuscript Received September 17, 1997[⊗]

A new open-framework manganese−gallium phosphate has been synthesized under solvothermal conditions and characterized by single-crystal XRD, thermogravimetric analysis, and magnetic susceptibility measurements [crystal data: $[MnGa(PO_3OH)_2(PO_4)][C_6N_2H_{14}]$, $M_r = 525.76$, monoclinic, space group $P2_1/n$ (No. 14), $a = 10.193(1)$, $b = 14.276(1)$, and $c = 10.380(1)$ Å, $\beta = 91.184(8)°$, $V = 1510$ Å^3, $Z = 4$, $R = 5.8\%$, $R_w = 7.8\%$ (2331 observed data with $I > 3\sigma(I)$)]. The structure consists of MnO_5, GaO_4, and PO_4 units linked to form a three-dimensional microporous framework encapsulating 1,4-diazabicyclo[2.2.2]octane cations. The Mn^{2+} ions have distorted square-pyramidal geometry and exist in $Mn_2(HPO_4)_4$ units within the framework. Antiferromagnetic ordering at $T_N = 10(1)$ K is ascribed to coupling between Mn^{2+} ions in these subunits, and the temperature dependence of the susceptibility can be successfully fitted assuming a Heisenberg exchange interaction ($J = -2.07(1)$ cm^{-1}, $g = 2.25(1)$). At higher temperatures (>70 K) Curie−Weiss paramagnetism is observed ($\theta = -20.2(2)$ K, $\mu_{eff} = 6.69(1)\mu_B$).

Introduction

The study of open-framework metal phosphates remains an active area of research because the materials have potential applications as molecular sieves, ion-exchangers, and catalysts. The phosphates of aluminium and gallium are of particular interest since they show a wide structural diversity. Many have framework topologies analogous to zeolites, while others have unique structures. For example, AlPO-17[1] and GaPO-34[2] are isostructural with the zeolites erionite and chabazite, respectively, while AlPO-18[3] and cloverite[4] have unique framework topologies.

The incorporation of heteroatoms into existing phosphate frameworks leads to the modification of the physical and chemical properties of the parent compounds. For example, the replacement of Al^{III} by a metal with lower valency produces an anionic framework which requires the presence of cations, commonly protonated organic species, in the pores or channels for charge compensation. Thus, the partial replacement of Al^{III} by M^{II} to give MAPOs (where M = Be, Mg, Zn, most first-row transition metals) can lead to new solid acids with enhanced catalytic properties. For example, CrAPO-5 is an effective catalyst for the oxidation of secondary alcohols,[5] and CoAPO-18 catalyses the conversion of methanol into light hydrocarbons.[6]

We have recently discussed the preparation of heterometal-containing open-framework gallium phosphates in ethylene glycol[7] and have characterized a number of substituted GaPOs including $[C_5NH_6][MGa_2P_3O_{12}]$ (M = Co, Fe, Mn, Zn),[7,8] $[C_3N_2H_5][MGa_2P_3O_{12}]$ (M = Co, Fe, Mn),[9] $[C_4NH_{10}][MGaP_2O_8]$ (M = Co, Zn),[7,10] and $[C_6N_2H_{14}]_2[Co_4Ga_5P_9O_{36}]$.[11] Here, we report the synthesis, structural and magnetic characterization of a new open-framework manganese−gallium phosphate, $[MnGa(PO_3OH)_2(PO_4)][C_6N_2H_{14}]$ (denoted MnGaPO-2), incorporating 1,4-diazabicyclo-[2.2.2]octane (DABCO) as the organic counterion.

Experimental Section

Synthesis and Initial Characterization. The title compound $[MnGa(PO_3OH)_2(PO_4)][C_6N_2H_{14}]$ was synthesized either as a pure polycrystalline phase (reaction (i)) or as single crystals (reaction (ii)) from predominantly nonaqueous systems under solvothermal condi-

[⊗] Abstract published in *Advance ACS Abstracts,* November 15, 1997.

(1) Pluth, J. J.; Smith, J. V.; Bennett, J. M. *Acta Crystallogr.* **1986**, *C42*, 283.
(2) Schott-Darie, C.; Kessler, H.; Soulard, M.; Gramlich, V.; Benazzi, E. *Stud. Surf. Sci. Catal.* (Zeolites and Related Microporous Materials: State of the Art 1994) **1994**, *84*, 101.
(3) Simmen, A.; McCusker, L. B.; Baerlocher, Ch.; Meier, W. M. *Zeolites* **1991**, *11*, 654.
(4) Estermann, M.; McCusker, L. B.; Baerlocher, Ch.; Merrouche, A.; Kessler, H. *Nature* **1991**, *352*, 320.
(5) Chen, J.; Dakka, J.; Neelman, E.; Sheldon, R. A. *J. Chem. Soc., Chem. Commun.* **1993**, 1379.
(6) Thomas, J. M.; Greaves, G. N.; Sankar, G.; Wright, P. A.; Chen, J.; Dent, A. J.; Marchese, L. *Angew. Chem., Int. Ed. Engl.* **1994**, *33*, 1871.
(7) Chippindale, A. M.; Cowley, A. R., accepted for publication in *Microporous Materials.*
(8) Chippindale, A. M.; Walton, R. I. *J. Chem. Soc., Chem. Commun.* **1994**, 2453.
(9) Bond, A. D.; Chippindale, A. M.; Cowley, A. R.; Powell, A. V.; Readman, J. E. accepted for publication in *Zeolites*, 1997.
(10) Chippindale, A. M.; Cowley, A. R. *J. Chem Soc., Chem. Commun.* **1996**, 673.
(11) Chippindale, A. M.; Cowley, A. R. *Zeolites* **1997**, *18*, 176.

S0897-4756(97)00162-2 CCC: $14.00

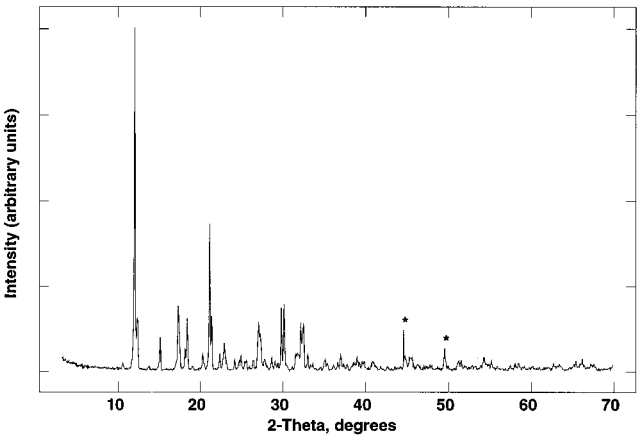

Figure 1. Powder X-ray diffraction pattern (Cu Kα radiation) of the title compound. (Note: peaks labeled * correspond to reflections from the aluminum sample holder).

tions. In reaction (i), Ga_2O_3 (0.4 g), $MnCl_2 \cdot 4H_2O$ (0.88 g), and 1,4-diazabicyclo[2.2.2]octane (DABCO) (3.35 g) were dispersed in 5.95 cm^3 of ethylene glycol by stirring. Orthophosphoric acid (2.35 cm^3, 85 wt %) was then added with further stirring to give a gel with overall composition Ga_2O_3:2.1$MnCl_2 \cdot 4H_2O$:16H_3PO_4:50$HOCH_2CH_2OH$:14DABCO. The gel was stirred until homogeneous, sealed in a Teflon-lined stainless steel autoclave, and heated at 433 K for 7 days. The solid product was collected by filtration, washed with distilled water, and left to dry overnight in air at 343 K. Examination of the product under the optical microscope showed it to be colorless and polycrystalline. X-ray powder diffraction analysis of the ground sample was performed on a Philips PW1710 diffractometer using Cu Kα radiation (λ = 1.540 60 Å). All peaks in the powder X-ray diffraction pattern (Figure 1) could be indexed on the basis of the monoclinic cell proposed for the title compound with refined lattice parameters a = 10.198(4), b = 14.276(4), and c = 10.374 (3) Å, β = 91.18(3)°.

Combustion analysis of the pure polycrystalline phase from reaction (i) gave the following results: C, 13.56; H, 3.04; N, 5.23, with no detectable chlorine. These compare well with the values calculated from the proposed formula $[MnGa(PO_3OH)_2(PO_4)][C_6N_2H_{14}]$: C, 13.70; H, 3.07; N, 5.33.

Energy-dispersive X-ray emission analysis of a finely ground sample of the product from reaction (i) was carried out on a JEOL 2000FX analytical electron microscope using $Mn_2P_2O_7$ and $GaPO_4$ as calibration standards. This showed the sample to be monophasic. No crystallites were observed containing either chlorine or just manganese, precluding the presence of manganese chloride or oxide phases (the oxygen content cannot be determined from the electron microscopy measurements). From the analysis of 20 crystallites, the average P:Mn ratio was found to be 3.01(23), the average P:Ga ratio 2.84(25), and the average Ga:Mn ratio 1.07(12). The results are in good agreement with the proposed formula $[MnGa(PO_3OH)_2(PO_4)][C_6N_2H_{14}]$.

Thermogravimetric analysis (TGA) of the product from reaction (i), performed under a flow of nitrogen gas on a Stanton Redcroft STA1500 thermal analyzer over the range 293−973 K at a heating rate of 10 K per minute, showed a gradual weight loss over the range 593−773 K. The total observed weight loss was ∼19%, compared with the calculated value of 21% for complete removal of the organic species. A powder X-ray diffraction pattern of the black product indicated that it was amorphous.

Magnetic susceptibility measurements on a bulk sample from reaction (i) were made using a Quantum Design MPMS2 SQUID susceptometer. Samples were loaded into gelatin capsules at room temperature and data collected over the temperature range 2≤ T≤ 340 K, both after cooling the sample in zero applied field (zfc) and after cooling in the measured field (fc) of 1 kG. Data were corrected for the diamagnetism of the gelatin capsule and for intrinsic core diamagnetism. Plots of the molar magnetic susceptibility (χ_{mol}) and reciprocal molar magnetic susceptibility vs temperature are shown in Figures 2a and 2b, respectively. The zfc and fc susceptibilities overlie each other at all temperatures, and an antiferromagnetic transition with a Néel temperature of 10(1) K is observed. Magnetic susceptibility data in the temperature range 70 ≤ T≤ 340 K can be fitted to a Curie−Weiss law with derived parameters θ = −20.2(2) K and C = 5.60(2) emu. The latter corresponds to an effective magnetic moment of 6.69(1)μ_B per manganese cation.

Single crystals suitable for X-ray analysis were obtained from reaction (ii) by a synthetic procedure similar to that for reaction (i) but using a gel of composition Ga_2O_3:1.2$MnCl_2 \cdot 4H_2O$:14H_3PO_4:50$HOCH_2CH_2OH$:0.3$Si(OEt)_4$:14DABCO. The tetraorthosilicate was added to the mixture as it has previously been found to aid crystal growth in gallium−phosphate syntheses.[12] The present synthesis produced crystals in the form of large colorless blocks and white polycrystalline material. The crystals have been found to be air and moisture stable over a period of at least 3 months. The powder X-ray diffraction pattern of a ground sample of the product showed that $[MnGa(PO_3OH)_2(PO_4)][C_6N_2H_{14}]$ was the predominant phase. The white polycrystalline material, an as-yet unidentified gallium phosphate, can also be prepared as the major product from a gel with a similar composition to that of reaction (ii) with the omission of $MnCl_2 \cdot 4H_2O$. Energy-dispersive X-ray emission analysis of this material gave an average P:Ga ratio of 1.15(7). C, H, and N analysis gave the following results: C, 17.10; H, 4.45; N, 6.08.

Crystal Structure Determination. A suitable crystal was selected from the product of reaction (ii) and mounted on a thin glass fiber using cyanoacrylate glue. X-ray data were collected at 293 K using an Enraf-Nonius CAD4 diffractometer (graphite-monochromated Cu Kα radiation, λ = 1.5418 Å). Lattice parameters (a = 10.193(1), b = 14.276(1), and c = 10.380(1) Å, β = 91.18(1)°) were determined for the monoclinic unit cell from 22 well-centered reflections (7.57 ≤ θ ≤ 15.10°). Intensity data were collected using the $\omega-2\theta$ scan technique over the range (0 ≤ θ ≤ 74°). Three standard reflections were measured every hour during the data collection, and no intensity variations were observed. Data were corrected for absorption using ψ-scans[13] and further corrected for Lorentz and polarization effects.[14] On the basis of the systematic absence conditions in the reduced data ($h0l$, $h+l$ odd; $0k0$, k odd), the space group was determined to be $P2_1/n$ (nonstandard setting of No.

(12) Kan, Q.; Glasser, F.; Xu, R. *J. Mater. Chem.* **1993**, *3*, 983.
(13) North, A. C. T.; Phillips, D. C.; Matthews, F. S. *Acta Crystallogr.* **1968**, *A24*, 351.
(14) Watkin, D. J.; Prout, C. K.; Lilley, P. M. deQ. RC93 User Guide, Chemical Crystallography Laboratory, University of Oxford, Oxford, U.K., 1994.

Table 1. Crystallographic Data for $[MnGa(PO_3OH)_2(PO_4)][C_6N_2H_{14}]$

formula	$[MnGa(PO_3OH)_2(PO_4)][C_6N_2H_{14}]$
M_r	525.76
crystal size (mm)	0.08 × 0.064 × 0.128
crystal habit	colorless block
crystal system	monoclinic
space group	$P2_1/n$ (No. 14)
a (Å)	10.193(1)
b (Å)	14.276(1)
c (Å)	10.380(1)
β (°)	91.184(8)
cell volume (Å^3)	1510.1
Z	4
ρ_{calc} (g cm^{-3})	2.31
μ (cm^{-1})	128.06
unique data	3773
observed data ($I > 3\sigma(I)$)	2331
R_{merg}	0.032
no. of params refined	233
R, R_w	0.058, 0.078[a]

[a] Refinement against F.

Table 2. Atomic Positional Parameters and Isotropic Thermal Parameters (Å^2) for $[MnGa(PO_3OH)_2(PO_4)][C_6N_2H_{14}]$

atom	x	y	z	U(iso)
Ga(1)	0.11141(6)	0.60674(4)	0.60391(5)	0.0205
Mn(1)	−0.11111(8)	0.99232(5)	0.62358(8)	0.0191
P(1)	0.3153(1)	0.50915(9)	0.7899(1)	0.0208
P(2)	−0.1144(1)	0.48092(8)	0.6739(1)	0.0201
P(3)	0.0219(1)	0.80083(9)	0.5019(1)	0.0214
O(1)	0.1222(4)	0.7282(3)	0.5589(4)	0.0272
O(2)	0.2407(4)	0.5921(3)	0.7266(4)	0.0268
O(3)	−0.0436(4)	0.5780(2)	0.6774(4)	0.0275
O(4)	0.3191(5)	0.5218(3)	0.9315(4)	0.0320
O(5)	0.4489(4)	0.4975(3)	0.7310(4)	0.0291
O(6)	0.2388(4)	0.4172(3)	0.7509(4)	0.0313
O(7)	−0.0513(4)	0.8481(3)	0.6074(4)	0.0298
O(8)	−0.0163(4)	0.4046(3)	0.7143(4)	0.0285
O(9)	−0.2319(4)	0.4835(3)	0.7559(4)	0.0336
O(10)	0.1564(4)	0.5343(3)	0.4684(3)	0.0273
O(11)	0.0927(4)	0.8627(3)	0.4094(4)	0.0296
O(12)	−0.0825(4)	0.7381(3)	0.4257(4)	0.0331
N(1)	0.9510(5)	0.2869(3)	−0.0897(4)	0.0289
N(2)	0.9515(5)	0.1625(3)	0.0775(5)	0.0309
C(1)	0.9233(8)	0.3288(5)	0.0371(6)	0.0455
C(2)	0.9083(7)	0.2501(4)	0.1351(6)	0.0336
C(3)	0.8440(8)	0.2182(5)	−0.1215(6)	0.0446
C(4)	0.8578(7)	0.1355(5)	−0.0303(6)	0.0392
C(5)	1.0805(8)	0.2386(6)	−0.0896(9)	0.0481
C(6)	1.0863(7)	0.1697(5)	0.0230(7)	0.0449
H(100)	−0.050(6)	0.690(4)	0.377(4)	0.05
H(101)	0.144(4)	0.409(5)	0.749(4)	0.05

Table 3. Selected Bond Distances (Å) for $[MnGa(PO_3OH)_2(PO)_4][C_6N_2H_{14}]$

Ga(1)−O(1)	1.800(4)	P(1)−O(2)	1.547(4)
Ga(1)−O(2)	1.825(4)	P(1)−O(4)	1.480(4)
Ga(1)−O(3)	1.817(4)	P(1)−O(5)	1.513(5)
Ga(1)−O(10)	1.812(4)	P(1)−O(6)	1.574(4)
Mn(1)−O(4)	2.112(4)	P(2)−O(3)	1.562(4)
Mn(1)−O(5)	2.217(4)	P(2)−O(8)	1.532(4)
Mn(1)−O(7)	2.154(4)	P(2)−O(9)	1.484(5)
Mn(1)−O(9)	2.056(5)	P(2)−O(10)	1.544(4)
Mn(1)−O(11)	2.107(4)		
		P(3)−O(1)	1.563(4)
N(1)−C(1)	1.477(8)	P(3)−O(7)	1.499(4)
N(1)−C(3)	1.498(9)	P(3)−O(11)	1.500(4)
N(1)−C(5)	1.490(8)	P(3)−O(12)	1.589(4)
N(2)−C(2)	1.458(8)		
N(2)−C(4)	1.507(8)	O(6)−H(101)	0.97(4)[a]
N(2)−C(6)	1.501(9)	O(12)−H(100)	0.93(4)[a]
C(1)−C(2)	1.525(9)		
C(3)−C(4)	1.52(1)		
C(5)−C(6)	1.527(9)		

[a] Included as chemical restraint.

Table 4. Selected Bond Angles (deg) for $[MnGa(PO_3OH)_2(PO_4)][C_6N_2H_{14}]$

O(1)−Ga(1)−O(2)	104.1(2)	Ga(1)−O(1)−P(3)	134.0(2)
O(1)−Ga(1)−O(3)	112.7(2)	Ga(1)−O(2)−P(1)	136.5(2)
O(2)−Ga(1)−O(3)	107.6(2)	Ga(1)−O(3)−P(2)	126.6(2)
O(1)−Ga(1)−O(10)	109.3(2)	Ga(1)−O(10)−P(2)	138.8(2)
O(2)−Ga(1)−O(10	106.6(2)		
O(3)−Ga(1)−O(10)	115.7(2)	Mn(1)−O(4)−P(1)	157.9(3)
		Mn(1)−O(5)−P(1)	113.2(2)
O(4)−Mn(1)−O(5)	151.3(2)	Mn(1)−O(7)−P(3)	129.3(2)
O(4)−Mn(1)−O(7)	85.7(2)	Mn(1)−O(9)−P(2)	176.7(3)
O(5)−Mn(1)−O(7)	82.9(1)	Mn(1)−O(11)−P(3)	136.7(3)
O(4)−Mn(1)−O(9)	108.5(2)		
O(5)−Mn(1)−O(9)	99.6(2)	O(2)−P(1)−O(4)	109.3(2)
O(7)−Mn(1)−O(9)	102.4(2)	O(2)−P(1)−O(5)	110.6(2)
O(4)−Mn(1)−O(11)	88.3(2)	O(4)−P(1)−O(5)	114.2(2)
O(5)−Mn(1)−O(11)	90.6(2)	O(2)−P(1)−O(6)	107.0(2)
O(7)−Mn(1)−O(11)	154.1(2)	O(4)−P(1)−O(6)	111.0(3)
O(9)−Mn(1)−O(11)	103.4(2)	O(5)−P(1)−O(6)	104.5(2)
C(1)−N(1)−C(3)	108.0(5)	O(3)−P(2)−O(8)	109.0(2)
C(1)−N(1)−C(5)	111.9(6)	O(3)−P(2)−O(9)	110.0(2)
C(3)−N(1)−C(5)	109.8(6)	O(8)−P(2)−O(9)	113.0(2)
C(2)−N(2)−C(4)	109.4(5)	O(3)−P(2)−O(10)	105.4(2)
C(2)−N(2)−C(6)	112.5(5)	O(8)−P(2)−O(10)	109.1(2)
C(4)−N(2)−C(6)	108.0(5)	O(9)−P(2)−O(10)	109.9(2)
N(1)−C(1)−C(2)	108.7(5)		
N(2)−C(2)−C(1)	108.8(5)	O(1)−P(3)−O(7)	110.7(2)
N(1)−C(3)−C(4)	108.3(5)	O(1)−P(3)−O(11)	108.2(2)
N(2)−C(4)−C(3)	108.2(5)	O(7)−P(3)−O(11)	117.1(2)
N(1)−C(5)−C(6)	108.6(6)	O(1)−P(3)−O(12)	103.9(2)
N(2)−C(6)−C(5)	108.1(5)	O(7)−P(3)−O(12)	106.2(2)
		O(11)−P(3)−O(12)	109.8(2)

14).[15] The structure was solved by direct methods using the program SHELXS-86,[16] and all framework metal, phosphorus, and oxygen atoms were located. The template carbon and nitrogen atoms and framework hydrogen atoms were then progressively located in difference Fourier maps. All Fourier calculations and subsequent full-matrix least-squares refinements were carried out using the CRYSTALS suite of programs.[17]

The structure contains two distinct metal sites, one 4-coordinate and one 5-coordinate. These were identified as gallium and manganese sites respectively on the basis of their differing thermal parameters. This assignment was subsequently verified by bond-valence calculations[18] which showed the manganese valence to be 2.02 and the gallium valence to be 3.19 on the 5- and 4-coordinate sites, respectively. This does not however preclude the possibility of a small degree of disorder of the metal atoms over the two sites, which would be unobservable using X-rays. The template hydrogen atoms were placed geometrically after each cycle of refinement, but the framework hydrogen coordinates were refined with H−O bond lengths restrained to be 1.00(5) Å and isotropic thermal parameters fixed at 0.05 Å^2. The data were corrected for extinction by the method of Larsen.[19] In the final cycle, 233 parameters were refined, including anisotropic thermal parameters for all non-hydrogen atoms, and a three-term Chebyshev

(15) *International Tables for X-ray Crystallography*; Hahn, T., Ed.; Kluwer Academic Publishers: Dordrecht, 1992; Vol. A.
(16) Sheldrick, G. M. SHELXS-86 Program for Crystal Structure Determination, University of Cambridge, 1986.
(17) Watkin, D. J.; Carruthers, J. R.; Betteridge, P. W. CRYSTALS User Guide, Chemical Crystallography Laboratory, University of Oxford, Oxford, U.K., 1985.
(18) Brese, N. E.; O'Keefe, M. O. *Acta Crystallogr.* **1991**, *B47*, 192.
(19) Larsen, A. C. *Acta Crystallogr.* **1967**, *23*, 664.

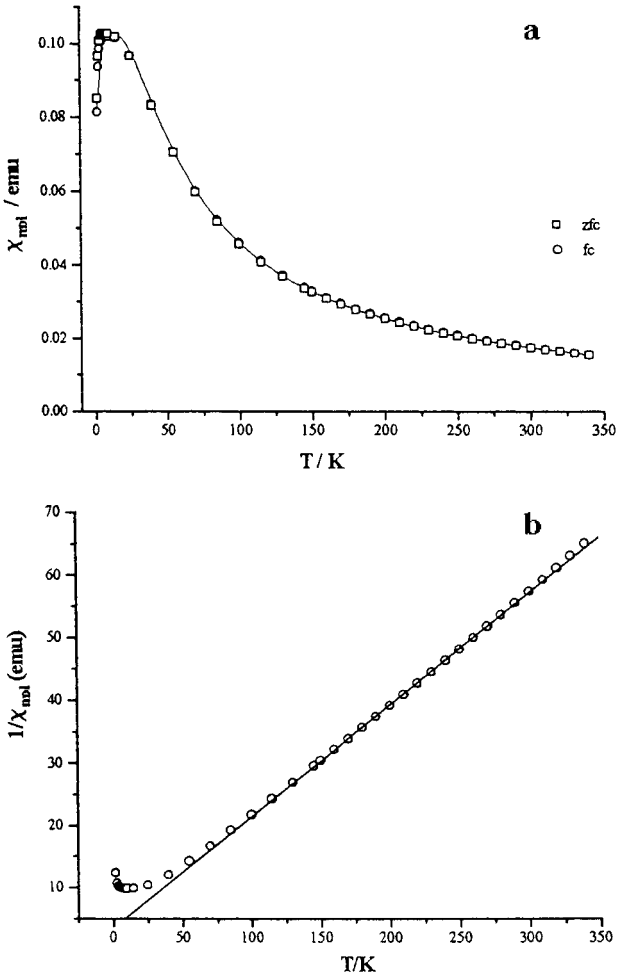

Figure 2. (a) Temperature dependence of the field-cooled (fc) and zero field-cooled (zfc) molar magnetic susceptibility of the title compound. The solid line represents the fit to the field-cooled susceptibility using the equation given in the text. (b) Reciprocal molar magnetic susceptibility. Points represent field-cooled data and the straight line represents the linear fit over the temperature range $70 \leq T \leq 340$ K.

polynomial was applied as weighting scheme.[20] The refinement converged to give $R = 0.058$ and $R_w = 0.078$. The crystallographic data are summarized in Table 1. Atomic coordinates, bond distances, and selected bond angles are given in Tables 2, 3, and 4, respectively, and the local coordination of the framework atoms are shown in Figure 3.

Crystal Structure

The structure consists of PO_4, GaO_4, and MnO_5 units linked to form a three-dimensional microporous framework. There are three crystallographically distinct phosphorus atoms, each of which are tetrahedrally coordinated and linked through oxygen to three adjacent metal atoms (P(1)−O_{av} = 1.51, P(2)−O_{av} = 1.53, P(3)−O_{av} = 1.52 Å). For two of the three phosphorus atoms, the fourth P−O bond length is significantly longer than the other three (P(1)−O(6) = 1.575(4), P(3)−O(12) = 1.589(4) Å), suggesting that these oxygen atoms are protonated. This was confirmed by the location of the hydrogen atoms in difference Fourier maps. The uncoordinated oxygen atom of the third phosphate group, P(2)O_4, is relatively close to the phosphorus atom (P(2)−O(8) = 1.532(4) Å), suggesting it to be unprotonated.

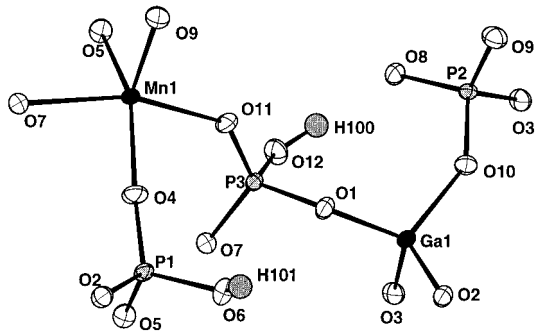

Figure 3. Local coordination of the MnGaPO-2 framework atoms showing the atom-labeling scheme and ellipsoids at 50% probability (drawing package CAMERON[21]).

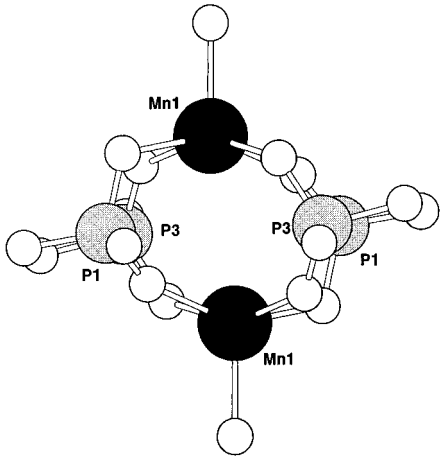

Figure 4. View of the $Mn_2(HPO_4)_4$ units. The Mn···Mn separation at 293 K is 3.465(2) Å (drawing package ATOMS[24]).

The GaO_4 units have tetrahedral geometry with a mean Ga−O bond length of 1.81 Å, a value typical of those found in other gallium phosphates.[22,23] The MnO_5 units have a slightly distorted square-pyramidal geometry, an unusual coordination for Mn^{2+}. Three of the four equatorial Mn−O bond lengths are similar (Mn(1)−O(4) = 2.112(4), Mn(1)−O(7) = 2.154(4), Mn(1)−O(11) = 2.107(4) Å), while the fourth is rather longer (Mn(1)−O(5) = 2.217(4) Å). This difference in bond lengths is due to the effects of hydrogen bonding as described below. The axial Mn−O bond length is shorter than all of these (Mn(1)−O(9) = 2.056(5) Å).

The MnO_5 units are linked in pairs by four HPO_4 groups to form $Mn_2(HPO_4)_4$ units in which the Mn···Mn distance is 3.465(2) Å (Figure 4). The $Mn_2(HPO_4)_4$ units are then linked via GaO_4 and PO_4 groups to form an extended anionic framework structure of formula $[MnGa(PO_3OH)_2(PO_4)]^{2-}$ (Figure 5). There are three distinct sets of pores passing through this framework. One set of pores runs parallel to the *b*-axis (Figure 6a) and is enclosed by elliptical 8-membered rings with cross-pore O···O distances of 4.93(1) × 7.09(1) Å. A second set of pores runs parallel to the vector [101] and is also enclosed by elliptical 8-membered rings (cross-pore O···O distances of 5.70(1) × 7.03(1) Å) (Figure 6b). A third set of pores running parallel to the vector [10−

(20) Carruthers, J. R.; Watkin, D. J. *Acta Crystallogr.* **1979**, *A35*, 698.

(21) Pearce, L. J.; Prout, C. K.; Watkin, D. J. CAMERON User Guide, Chemical Crystallography Laboratory, University of Oxford, Oxford, U.K., 1993.

(22) Parise, J. B. *Acta Crystallogr.* **1986**, *C42*, 283.

(23) Parise, J. B. *Inorg. Chem.* **1985**, *24*, 4312.

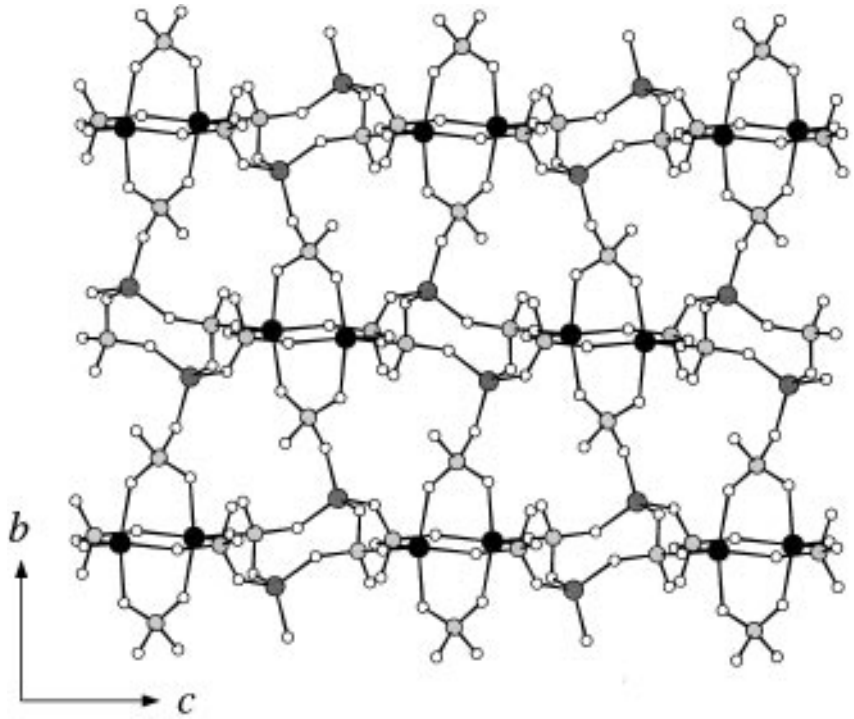

Figure 5. View along the *a* axis showing the linkage of the MnO_5, GaO_4, and PO_4 units to form an extended anionic framework structure. Key: large black spheres = manganese, large shaded spheres = gallium, small shaded spheres = phosphorus, open spheres = oxygen. Framework hydrogens and DABCO molecules have been omitted for clarity (drawing package CAMERON[21]).

1] is enclosed by highly irregular 10-membered rings (Figure 6c) and partially obstructed by projecting P−OH groups. The latter pores have typical O···O distances of 5.30(1) × 3.27(1) Å. The three sets of channels intersect to form an extended three-dimensional pore network.

The inorganic framework has a net charge of −2 per formula unit. Charge balance is achieved by the presence of ordered $[C_6N_2H_{14}]^{2+}$ template cations, which reside within the pore network and are hydrogen bonded to the framework. One of the template N−H groups is hydrogen-bonded to the uncoordinated oxygen of the $P(2)O_4$ group (N(1)···O(8) = 2.665(6) Å) and the second N−H group is hydrogen-bonded to one of the equatorial oxygens of the MnO_5 unit (N(2)···O(5) = 2.785(6) Å). The latter interaction results in an elongation of the Mn(1)−O(5) bond as mentioned previously, but no significant elongation of the P(1)−O(5) bond. There are also strong intraframework hydrogen-bonded interactions involving the P(1)OH and P(3)OH groups and the P(2)O(8) group (O(6)···O(8) = 2.626(6), O(12)···O(8) = 2.708(6) Å).

Discussion of Magnetic Data

The effective magnetic moment derived from the fit to the Curie−Weiss law indicates that the manganese cations are present as high-spin Mn^{2+}, although the moment itself is higher than that calculated on the basis of the spin-only formula ($5.92\mu_B$). While this high value *could* arise from the presence of a paramagnetic impurity, high concentrations of this secondary phase would be required to produce the observed increase in magnetic moment. No evidence has been found from the analysis results for such an additional phase. A more likely explanation is that the high-temperature limit for data collection attainable by the SQUID susceptometer used in this work is insufficiently high for the moments to be noninteracting. Short-range ferromagnetic interactions would lead to an increase in measured susceptibility and hence a higher effective magnetic moment. The structure determined by single-crystal XRD shows that HPO_4 groups link pairs of Mn^{2+} ions, each in a distorted square-pyramidal coordination environment, to form a structural subunit in which the Mn^{2+} ions are only ca. 3.5 Å apart (Figure 4). This suggests that the observed antiferromagnetism of $[MnGa(PO_3OH)_2(PO_4)][C_6N_2H_{14}]$ is the result of antiferromagnetic coupling between pairs of Mn^{2+} ions in this dimeric subunit, similar to that observed in other Mn-bridged dinuclear complexes.[25,26,27] The next-nearest neighbors of each Mn^{2+} ion are over 8 Å away; too great a distance for significant short-range ferromagnetic interactions. However, the latter could arise from slight disordering of the Mn and Ga over the metal sites which would then provide a Mn−O−P−O−Mn superexchange pathway. Such disorder is not readily detectable by X-ray diffraction methods.

Assuming an exchange Hamiltonian of the form $-2JS_1 \cdot S_2$ for the coupling between two ions with spins $S_1 = S_2 = {}^5/_2$, the magnetic susceptibility per ion is given by:

$$\chi_1 = \frac{Ng^2\mu_B{}^2[\exp(28x) + 5\exp(24x) + 14\exp(18x) + 30\exp(10x) + 55]}{kT[\exp(30x) + 3\exp(28x) + 5\exp(24x) + 7\exp(18x) + 9\exp(10x) + 11]}$$

where $x = (-J/kT)$.

To allow for the possibility of a paramagnetic impurity, a Curie-like term (proportional to $1/T$) was included in the expression for the molar magnetic

(24) Dowty, E. ATOMS for Windows, Shape Software, 521 Hidden Valley Road, Kingsport, TN 37663, 1995.
(25) Sakiyama, H.; Tokuyama, K.; Matsumara, Y.; Okawa, H. *J. Chem. Soc., Dalton Trans.* **1993**, 2329.
(26) Nepveu, F.; Gaultier, N.; Korber, N.; Jaud, J.; Castan, P. *J. Chem. Soc., Dalton Trans.* **1995**, 4005.
(27) Cano, J.; De Munno, G.; Sanz, J.; Ruiz, R.; Lloret, F.; Faus, J.; Julve, M. *J. Chem. Soc., Dalton Trans.* **1994**, 3465.

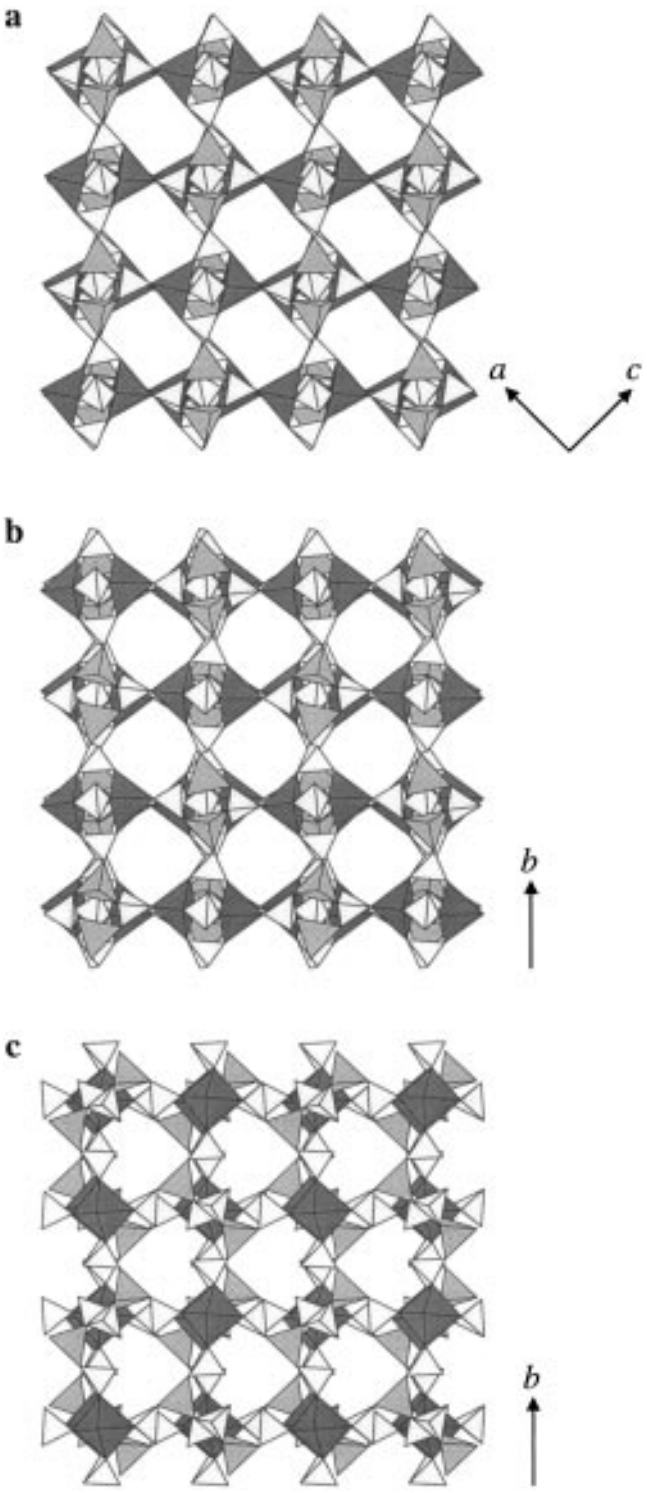

Figure 6. Polyhedral representation of the MnGaPO-2 framework viewed (a) along the *b* axis showing channels enclosed by 8-membered rings, (b) along the vector [101] showing 8-membered rings, and (c) along the vector [10−1] showing highly irregular 10-membered rings. Key: MnO_5 square pyramids = dark grey, GaO_4 tetrahedra = mid grey, PO_4 tetrahedra = light grey (drawing package ATOMS[24]).

susceptibility and experimental data were therefore fitted to the expression:

$$\chi_{mol} = (1 - f)\chi_1 + \frac{f(35Ng^2\mu_B{}^2)}{12kT}$$

The best fit was obtained with a *g* value of 2.25(1), a coupling constant, *J*, of −2.07(1) cm^{-1} with a mole fraction, *f*, of the paramagnetic phase of <0.015. This small mole fraction value is consistent with the analytical data. The molar magnetic susceptibility calculated with these parameters is shown as the solid line in Figure 2. Good agreement between measured and calculated data is obtained over the whole temperature range. This supports the suggestion that the predominant magnetic interaction is between pairs of Mn^{2+} ions which are linked by HPO_4 groups. The value of *J* determined in the present work indicates an antiferromagnetic interaction which can occur either through a complex Mn−O−P−O−Mn superexchange pathway or via a direct through-space interaction which may be favored by a lattice contraction on cooling. Neutron diffraction studies are currently in progress to determine the mechanism responsible for this magnetic behavior.

Although metal-substituted gallium phosphates form extended solids, their magnetic behavior may be traced to the dilution of a magnetic ion in a nonmagnetic gallium-phosphate lattice and is thus similar to that observed in transition-metal complexes. Dinuclear Mn^{II} oxy-bridged complexes in which Mn−Mn separations are of the order of 3.48 Å have been shown previously to have coupling constants in the range of −1.3 to −2.8 cm^{-1}.[25,26]

Conclusion

The compound described here, MnGaPO-2, has a framework topology unlike that of any previously characterized phase and is the second example of a manganese−gallium phosphate to be reported. The first, MnGaPO-1, has the laumontite structure and contains either pyridine or imidazole within the channels.[7,9] The manganese in the present material is found in a coordination geometry unusual for Mn^{2+} in extended solids. Although such square-pyramidal coordination has been reported previously in a number of molecular complexes, e.g. $((CF_3)_3C_6H_2O)_2Mn(THF)_3$,[28] the Cambridge Structural Database[29] contains no examples of complexes with this manganese geometry in the presence of phosphate ligands.

The three-dimensional pore network present within this material contains $[C_6N_2H_{14}]^{2+}$ cations. TGA measurements suggest that removal of the organic species may be facile, permitting the microporous nature of the material to be exploited, for example in catalytic applications.

Acknowledgment. A.V.P. and A.R.C. thank the EPSRC for support of the SQUID magnetometer (Grants GR/J36075 and GR/J34231) and for a studentship, respectively.

Supporting Information Available: Crystallographic data for MnGaPO-2 (18 pages). Ordering information is given on any current masthead page.

CM9701623

(28) Roesky, H. W.; Scholz, M.; Noltemeyer, M. *Chem. Ber.* **1990**, *123*, 2303.
(29) Cambridge Structural Database (v.2.3.7), Cambridge Crystallographic Data Centre, 12 Union Road, Cambridge CB2 1EZ, U.K., 1995.